ELSEVIER

Chemical Engineering Journal 141 (2008) 42–50

Chemical Engineering Journal

www.elsevier.com/locate/cej

Metal biosorption by algae *Gelidium* derived materials from binary solutions in a continuous stirred adsorber

Vítor J.P. Vilar, Cidália M.S. Botelho, Rui A.R. Boaventura *

LSRE-Laboratory of Separation and Reaction Engineering, Departamento de Engenharia Química, Faculdade de Engenharia da Universidade do Porto, Rua Dr. Roberto Frias, 4200-465 Porto, Portugal

Received 10 May 2007; received in revised form 27 July 2007; accepted 10 October 2007

Abstract

Continuous metal biosorption from Pb(II)/Cu(II) and Pb(II)/Cd(II) solutions onto algae *Gelidium* and granulated algal waste was performed in a continuous stirred tank adsorber (CSTA). Biosorption was simulated by a mass transfer model including intraparticle and film resistances and equilibrium described by the Langmuir binary equation. The breakthrough curves present an initial "knee" suggesting a film resistance to mass transfer. Biosorption of Pb(II) is significantly reduced by the presence of Cu(II), which indicates that competition exists for the same binding sites. In the binary system Pb(II)/Cd(II), an "overshoot" region was observed, for the cadmium concentration profile, due to the higher affinity of lead ions to the binding sites. A fast and efficient desorption of Cu(II) and Pb(II) was obtained using a 0.1 M HNO_3 solution, as eluent. Results suggest that desorption is based on ion exchange between the metal ions, loaded in the biomass, and H^+ in solution. Desorption was adequately predicted by a mass transfer model considering intraparticle diffusion resistance and equilibrium given by the mass action law.

Keywords: *Gelidium*; Composite material; Adsorption; Desorption; Mass transfer; Mathematical modelling

1. Introduction

Biosorption of metal ions has been reported to be an alternative technology to the conventional treatment of metal-bearing effluents [1,2]. Different kinds of low-cost sorbents have been applied with success in metal removal, as marine seaweed [3], wastes from industrial activities [4], bacteria [5], fungi [6] and others [7–9]. Such biomass is chemically complex and contains different active groups, with properties for binding other chemical substances or ions, after attracting them from solution.

Algae *Gelidium* and a granulated algal waste from the agar extraction industry have demonstrated the ability to efficiently remove metal ions from single-metal solutions in batch reactor, packed bed column and continuous stirred tank adsorbers at different pH, ionic strength and temperature conditions [10–14]. Industrial effluents are, in general, a mixture of different ionic species. Kinetic and equilibrium experiments have been also performed using different binary mixtures [10]. For the application of biosorption processes in large-scale, the development and design of continuous processes and the study of adsorbent selectivity in the presence of multi-metal systems are important contributions.

Metal biosorption from Pb/Cu, Pb/Ni and Pb/Cu/Ni solutions onto *Rhizopus arrhizus* in a continuous-flow stirred-tank contactor was predicted by a multi-component mathematical model based on mass balances for liquid and solid phases [15]. The relative capacities in the ternary metal mixtures were in the order Pb > Ni > Cu, in agreement with the single and dual component data [15]. Similar works were performed, using *Sphaerotilus natans* cells confined in a UF (Ultrafiltration)/MF (Microfiltration) membrane reactor [16,17]. The biosorption tests using single and binary metallic solutions (Cu, Pb and Cu–Pb) denoted a higher biomass affinity for Pb than for Cu.

In this work, the metal biosorption from Pb(II)/Cu(II) and Pb(II)/Cd(II) solutions has been studied using algae *Gelidium* and granulated algal waste as biosorbents, in a continuous stirred tank adsorber (CSTA). A mass transfer model was developed to describe the biosorption process, considering film resistance, intraparticle homogeneous diffusion and equilibrium described by the binary Langmuir isotherm. Elution from saturated biosorbents was carried out using a 0.1 M HNO_3 solution, as eluent.

* Corresponding author. Tel.: +351 225081683; fax: +351 225081674.
E-mail addresses: vilar@fe.up.pt (V.J.P. Vilar), cbotelho@fe.up.pt (C.M.S. Botelho), bventura@fe.up.pt (R.A.R. Boaventura).

1385-8947/$ – see front matter © 2007 Elsevier B.V. All rights reserved.
doi:10.1016/j.cej.2007.10.011

Nomenclature

a_p	specific area for thin plate particles (cm^{-1})
C_{AI}	metal concentration in the bulk solution at the beginning of the elution process (mg metal/l fluid)
C_{b_i}	metal concentration in the bulk for species i (mg or mmol metal/l fluid)
$C_{b_{i_0}}$	initial metal concentration in the bulk for species i (mg or mmol metal/l fluid)
C_{E_i}	feed concentration for species i (mg or mmol metal/l fluid)
C_{f_i}	metal concentration in the film (mg or mmol metal/l fluid)
$C_{final(i)}$	metal concentration in the solution at the end of the saturation or elution process (mg metal/l fluid)
C_H	equilibrium concentration of proton in the fluid phase (mmol proton/l fluid)
C_{M_i}	equilibrium concentration of metal i in the fluid phase (mmol metal/l fluid)
C_T	total (metals + protons) liquid concentration (mmol/l fluid)
C_{T_0}	initial total (metals + protons) liquid concentration (mmol/l fluid)
C_{T_E}	total feed (acid) liquid concentration (mmol/l fluid)
d_p	particle diameter (cm)
D_{h_i}	homogeneous diffusion coefficient for species i (cm^2/s)
k_{f_i}	film mass transfer coefficient for species i (cm/s)
k_{p_i}	mass transfer coefficient for intraparticle diffusion for species i (cm/s)
K_H	equilibrium proton constant (l fluid/mmol H)
K_{M_i}	equilibrium metal i constant (l fluid/mmol M)
K_i	equilibrium constant of Langmuir for species i (l fluid/mg M)
K_H^M	selectivity coefficient between ion M in the particle and H in solution
N_{d_i}	number of mass transfer units by intraparticle diffusion for species i
N_{f_i}	number of mass transfer units by film diffusion for species i
pH_{SE}	pH of feed solution
pH_{CI}	initial pH of the interstitial fluid inside the adsorber
pH_{CF}	final pH of the interstitial fluid inside the adsorber
$\langle q_i \rangle$	average metal i concentration in the solid phase (mg or mmol metal/g biomass)
q_H	equilibrium concentration of protons in the biomass (mmol metal/g biomass)
q_{M_i}	equilibrium concentration of metal i in the biomass (mg or mmol metal/g biomass)
q_{i_0}	metal i concentration in the solid phase after biomass saturation (mmol metal/g biomass)
q_i^*	metal i concentration in the solid phase in equilibrium with C_{f_i} for each species i (mg or mmol metal/g biomass)
Q	flow rate (cm^3/min)
Q_{max}	concentration of carboxylic groups or maximum capacity of biomass (mg or mmol/g biomass)
R	half of thickness of the thin plate (cm)
R^2	correlation coefficient
S_2^R	model residual variance
t	time (s)
T	temperature (°C)
V_r	adsorber volume capacity (cm^3)
W	mass of biosorbent (g)
$\langle y_i \rangle$	dimensionless average concentration in the solid phase for species i
y_{b_i}	dimensionless concentration in the fluid phase for species i
y_{f_i}	dimensionless concentration in the fluid phase at the film for species i
y_T	dimensionless total concentration in the fluid phase
y_i^*	dimensionless concentration in the solid phase at the particle surface for species i

Greek symbols

ε	adsorber porosity
τ	space time (s)
τ_{d_i}	time constant for intraparticle diffusion for species i
τ_{f_i}	time constant for film diffusion for species i
θ	dimensionless time
ρ_{ap}	apparent density of particles (g solid/cm^3 particle)
ξ_i	adsorber capacity factor for each species i in saturation
ξ'	adsorber capacity factor in desorption
$\alpha_1,\alpha_2,\beta_1,\beta_2,\gamma_1,\gamma_2,\psi$	constants of the mass transfer model

A mass transfer model, considering intraparticle diffusion and equilibrium described by the mass action law was successfully applied.

2. Materials and methods

2.1. Biosorbents

An algal waste from the agar extraction industry was immobilized in an organic polymer (Polyacrylonitrile, PAN) and used as biosorbent in this study, as well as algae *Gelidium*, the raw material for agar extraction. Algae *Gelidium sesquipedale* is a red algae, harvested in the coasts of Algarve and São Martinho do Porto, Portugal. Algal waste and algae *Gelidium* were dried at 60 °C in laboratory and then crushed in a mill (Retsch, model ZM 100). To prepare the composite particles, fibrous PAN was first dissolved in DMSO (dimethyl sulfoxide) during 1–2 h. The powdered active component (industrial algal waste) was gradually added to PAN solution under stirring and the suspension mixed for about 30 min. Homogeneous suspension was then dispersed

into water (coagulation bath) at room temperature. Beads formed in the water bath were washed with distilled water, separated by filtration on Buchner funnel and dried at about 30–40 °C. Dry product was then sieved. According to the procedure used, dry beads contain 75% of the active component. Physical and chemical characteristics and preparation of both materials were presented in previous works [11,14,18,19].

2.2. Metal solutions

Pb(II), Cd(II) and Cu(II) solutions were prepared by dissolving a weighed quantity of anhydrous lead(II) chloride (Sigma–Aldrich, 98%), anhydrous cadmium(II) chloride (Sigma–Aldrich, 99%) and copper(II) chloride dehydrate (Riedel-de Haën, 99%) in distilled water. pH was controlled by the addition of 0.01 M HCl and 0.01 M NaOH solutions.

2.3. Continuous adsorber experiments

CSTA experiments were conducted in a "Carberry" adsorber or hampers adsorber, perfectly mixed by mechanical stirring (Heidolph) with a useful volume of 540 cm^3. The CSTA was equipped with a jacket surrounding the adsorber body for temperature control. The apparent densities of the biosorbents were determined by mercury intrusion (PORESIZER 9320) as 1.34 and 0.25 g/cm^3, respectively for algae *Gelidium* and composite material [20].

A known quantity of algae *Gelidium* or composite material (≈10 g) was placed in the hampers. The binary metal solution was pumped through the CSTA at 35.5 ml/min flow rate using a peristaltic pump (Ismatec Ecoline VC-380). The flow rate was controlled during the experiments. Metal concentration in the CSTA effluent was determined and the pH of the effluent was continuously monitored. Metal saturated biomass was regenerated using a 0.1 M HNO_3 solution. Prior to the experiments, the CSTA was rinsed with a 20% HNO_3 solution and distilled water, to remove all contaminants.

2.4. Analytical procedure

Pb(II), Cd(II) and Cu(II) concentrations in solution were measured by Atomic Absorption Spectrometry (GBC 932 Plus AAS).

3. Theoretical approach

3.1. Equilibrium

A mathematical equilibrium model has been developed assuming the competition between metal ions and protons and that only one kind of active sites (carboxylic groups) exists in the cell wall, which are responsible for metal biosorption at pH < 7.0. The model defines apparent equilibrium binding constants, K_H and K_{M_i} for protons and divalent metal cations M_i, respectively, sorbing onto binding sites in biomass according to the following equation [10]:

$$q_{M_i} = \frac{Q_{max} K_{M_i} C_{M_i}}{1 + K_H C_H + \sum_{i=1}^{n} K_{M_i} C_{M_i}} \quad (1)$$

or

$$q_{M_i} = \frac{Q_{max} K_i C_{M_i}}{1 + \sum_{i=1}^{n} K_i C_{M_i}} \quad (2)$$

where

$$K_i = \frac{K_{M_i}}{1 + K_H C_H} \quad (3)$$

From K_H values it is possible to calculate the binary Langmuir equilibrium constant for each pH.

3.2. CSTA modelling

3.2.1. Saturation

Isothermal operation, adsorption equilibrium described by the binary Langmuir isotherm, external (film) resistance and internal mass transfer resistance described by the LDF (linear driving force) approximation have been assumed in modelling CSTA biosorption:

Mass conservation in the fluid around particles

$$Q C_{E_i} = Q C_{b_i} + \varepsilon V_r \frac{dC_{b_i}}{dt} + (1-\varepsilon) V_r \rho_{ap} \frac{d\langle q_i \rangle}{dt} \quad (4)$$

Mass conservation inside particles (LDF)

$$\frac{d\langle q_i \rangle}{dt} = k_{p_i} a_p [q_i^* - \langle q_i \rangle] \quad (5)$$

where $k_{p_i} a_p = 3 D_{h_i} / R^2$, considering a parabolic profile for the metal concentration inside the particle, and $a_p = 1/R$ the specific area for thin plate particles.

For no accumulation in the fluid film surrounding the particles:

$$k_{f_i} a_p (C_{b_i} - C_{f_i}) = \rho_{ap} \frac{d\langle q_i \rangle}{dt} \quad (6)$$

Equilibrium relationship:

$$q_i^* = \frac{Q_{max} K_i C_{f_i}}{1 + \sum_{i=1}^{2} K_i C_{f_i}} \quad (7)$$

Initial conditions can be described as:

$$t = 0, \quad C_{b_i} = 0, \quad C_{f_i} = 0, \quad \langle q_i \rangle = 0 \quad (8)$$

Introducing the dimensionless variables:

$$\theta = \frac{t}{\tau}, \quad y_{b_i} = \frac{C_{b_i}}{C_{E_i}}, \quad y_{f_i} = \frac{C_{f_i}}{C_{E_i}}, \quad \langle y_i \rangle = \frac{\langle q_i \rangle}{Q_{max}},$$

$$y_i^* = \frac{q_i^*}{Q_{max}}$$

and dimensionless parameters:

$$\tau = \frac{\varepsilon V_r}{Q}, \quad \xi_i = \frac{(1-\varepsilon)}{\varepsilon}\rho_{ap}\frac{Q_{max}}{C_{E_i}}, \quad \tau_{f_i} = \frac{\varepsilon}{(1-\varepsilon)}\frac{1}{k_{f_i}a_p},$$

$$N_{f_i} = \frac{\tau}{\tau_{f_i}}, \quad N_{d_i} = k_{p_i}a_p\tau$$

Eqs. (4)–(6) can be written in dimensionless form, respectively as:

$$\frac{dy_{b_i}}{d\theta} = 1 - y_{b_i} - \xi_i\frac{d\langle y_i\rangle}{d\theta} \tag{9}$$

$$\frac{d\langle y_i\rangle}{d\theta} = \frac{N_{f_i}}{\xi_i}(y_{b_i} - y_{f_i}) \tag{10}$$

$$\frac{d\langle y_i\rangle}{d\theta} = N_{d_i}(y_i^* - \langle y_i\rangle) \tag{11}$$

Equaling Eq. (10) to Eq. (11):

$$[y_{b_i} - y_{f_i}] = \frac{N_{d_i}\xi_i}{N_{f_i}}[y_i^* - \langle y_i\rangle] \tag{12}$$

And deriving Eq. (12) in order to time, we get:

$$\frac{dy_{b_i}}{d\theta} - \frac{dy_{f_i}}{d\theta} = \frac{N_{d_i}\xi_i}{N_{f_i}}\left[\sum_{i=1}^{2}\frac{\partial y_i^*}{\partial y_{f_i}}\frac{\partial y_{f_i}}{\partial\theta} - \frac{d\langle y_i\rangle}{d\theta}\right] \tag{13}$$

Solving the linear two variables system, gives:

$$\frac{dy_{f_1}}{d\theta} = \frac{[\gamma_1((d\langle y_1\rangle/d\theta) + (dy_{b_1}/d\theta))]\psi + [\gamma_2((d\langle y_2\rangle/d\theta) + (dy_{b_2}/d\theta))][(1+\gamma_1\alpha_1)\gamma_1\alpha_2]}{[1+\gamma_1\alpha_1+\gamma_2\beta_2+\gamma_1\gamma_2(\alpha_1\beta_2-\alpha_2\beta_1)](1+\gamma_1\alpha_1)} \tag{14}$$

$$\frac{dy_{f_2}}{d\theta} = \frac{[\gamma_1((d\langle y_1\rangle/d\theta) + (dy_{b_1}/da))](\gamma_2\beta_1) + [\gamma_2((d\langle y_2\rangle/d\theta) + (dy_{b_2}/da))](1+\gamma_1\alpha_1)}{[1+\gamma_1\alpha_1+\gamma_2\beta_2+\gamma_1\gamma_2(\alpha_1\beta_2-\alpha_2\beta_1)]} \tag{15}$$

with

$$\psi = 1 + \gamma_1\alpha_1 + \gamma_2\beta_2 + \gamma_1\gamma_2\alpha_1\beta_2 \tag{16}$$

$$\alpha_1 = \frac{K_1C_{E_1}(1+K_2C_{E_2}y_{f_2})}{(1+K_1C_{E_1}y_{f_1}+K_2C_{E_2}y_{f_2})^2};$$

$$\alpha_2 = \frac{K_1K_2C_{E_1}C_{E_2}y_{f_1}}{(1+K_1C_{E_1}y_{f_1}+K_2C_{E_2}y_{f_2})^2} \tag{17}$$

$$\beta_1 = \frac{K_1K_2C_{E_1}C_{E_2}y_{f_2}}{(1+K_1C_{E_1}y_{f_1}+K_2C_{E_2}y_{f_2})^2};$$

$$\beta_2 = \frac{K_2C_{E_2}(1+K_1C_{E_1}y_{f_1})}{(1+K_1C_{E_1}y_{f_1}+K_2C_{E_2}y_{f_2})^2} \tag{18}$$

and the initial conditions:

$$\theta = 0, \quad y_{b_i} = 0, \quad y_{f_i} = 0, \quad \langle y_i\rangle = 0 \tag{19}$$

The ODEs system, Eqs. (9)–(11) for the two metal ions and Eqs. (14) and (15) together with the initial conditions (Eq. (19)), were solved by LSODA subroutine [21].

3.2.2. Elution

Copper ions desorption can be achieved with a HNO_3 concentrated solution [18]. Desorption was considered as an ion exchange process, between metal ions and protons. The exchange rate was determined assuming a 1:1 stoichiometric exchange. Equilibrium desorption was described by the mass action law:

$$q_i^* = \frac{K_H^M\, Q_{max}\, C_{b_i}}{C_T + (K_H^M - 1)C_{b_I}} \tag{20}$$

where $K_H^M = 0.93$ and 1.1 and $Q_{max} = 0.36$ and 0.16 mmol/g, respectively, for algae *Gelidium* and composite material [18].

Isothermic operation, adsorption equilibrium described by the mass action law and internal mass transfer resistance described by the LDF approximation were assumed to model the elution process. It has been considered that the elution of one metal does not interfere in the elution of the other metal, and that the selectivity coefficient, K_H^M, is the same for both metals. Mass transfer external resistance has been neglected, since the ion-exchange process between the metal ions and protons is very fast, when using a strong acid eluent.

For a three-component system, the conservation of total concentration in the fluid phase, assuming that after saturation, metal ions and protons bound to the biomass are occupying the total of active sites, which implies that the partial derivative in time is zero ($d(\langle q_H\rangle + \langle q_M\rangle)/dt = dQ_{max}/dt = 0$, yields:

$$\frac{dy_T}{d\theta} = \frac{C_{T_E}}{C_{T_0}} - y_T \tag{21}$$

The new dimensionless variables are defined as:

$$y_T = \frac{C_T}{C_{T_0}}, \quad y_{b_i} = \frac{C_{b_i}}{C_{T_0}}$$

where C_T and C_{T_0} are the molar total (metals and protons) concentrations in the bulk solution at each time instant and at the end of the saturation process.

The dimensionless parameters are the same considered before, with the exception of the column capacity factor, which is now defined as:

$$\xi' = \frac{(1-\varepsilon)}{\varepsilon}\rho_{ap}\frac{Q_{max}}{C_{T_0}}$$

Applying the dimensionless variables to Eq. (20) gives:

$$y_i^* = \frac{K_H^M\, y_{b_i}}{y_T + (K_H^M - 1)\, y_{b_i}} \tag{22}$$

Initial conditions:

$$\theta = 0, \quad y_{b_i} = \frac{C_{b_{i_0}}}{C_{T_0}}, \quad y_T = 1, \quad \langle y_i \rangle = \frac{q_{i_0}}{Q_{max}} \tag{23}$$

The equations concerning mass conservation in the fluid for each metal ion, Eq. (9); total mass conservation in the fluid, Eq. (21); mass conservation in the particle for each metal ion, Eq. (11) with the initial conditions (Eq. (23)), were simultaneously solved by LSODA subroutine [21], where equilibrium is given by the mass action law, Eq. (22), for each metal ion.

4. Results and discussion

4.1. Biosorption equilibrium

Equilibrium results for metal biosorption from Pb/Cu and Pb/Cd solutions onto algae *Gelidium* and composite material were presented in a previous work [10]. Two equilibrium models were developed to describe the equilibrium results. The discrete model considers a homogeneous distribution of the carboxylic groups, taking into account the competition between metal ions and protons (Eq. (1)). For constant pH, Eq. (1) can be transformed in the binary Langmuir equation. The continuous model (NICA model [22]) considers an heterogeneous distribution of sites given by the Sips distribution [23]. The continuous model better describes the biosorption mechanism for all single and two-metal systems. Because of the complexity of the continuous model equation, the binary Langmuir equation has been used to represent the equilibrium in the mass transfer model. Fig. 1 (a_i) and (b_i) present the equilibrium surface for the systems Pb/Cu and Pb/Cd and both biosorbents. The discrete model parameters Eq. (1) are shown in Table 1 [10]. These values were obtained, considering the single-metal experimental data at pH 5.3, 4 and 3 for Cu and Pb and 6.5, 5.3 and 4 for the Cd, and the two-metal experiments (Pb/Cu and Pb/Cd) at pH 5.3. The obtained model parameters suggest that carboxylic groups have higher affinity to lead ions than for copper or cadmium ions. Copper has more influence than cadmium on lead adsorption.

4.2. Continuous biosorption

The operating conditions for the continuous experiments are presented in Table 2.

4.2.1. Biosorption from a Pb/Cu solution

Experimental results for metal ions biosorption from a Pb/Cu solution by algae *Gelidium* and composite material are presented in Fig. 2(a and b), respectively. As the inlet Cu(II) molar

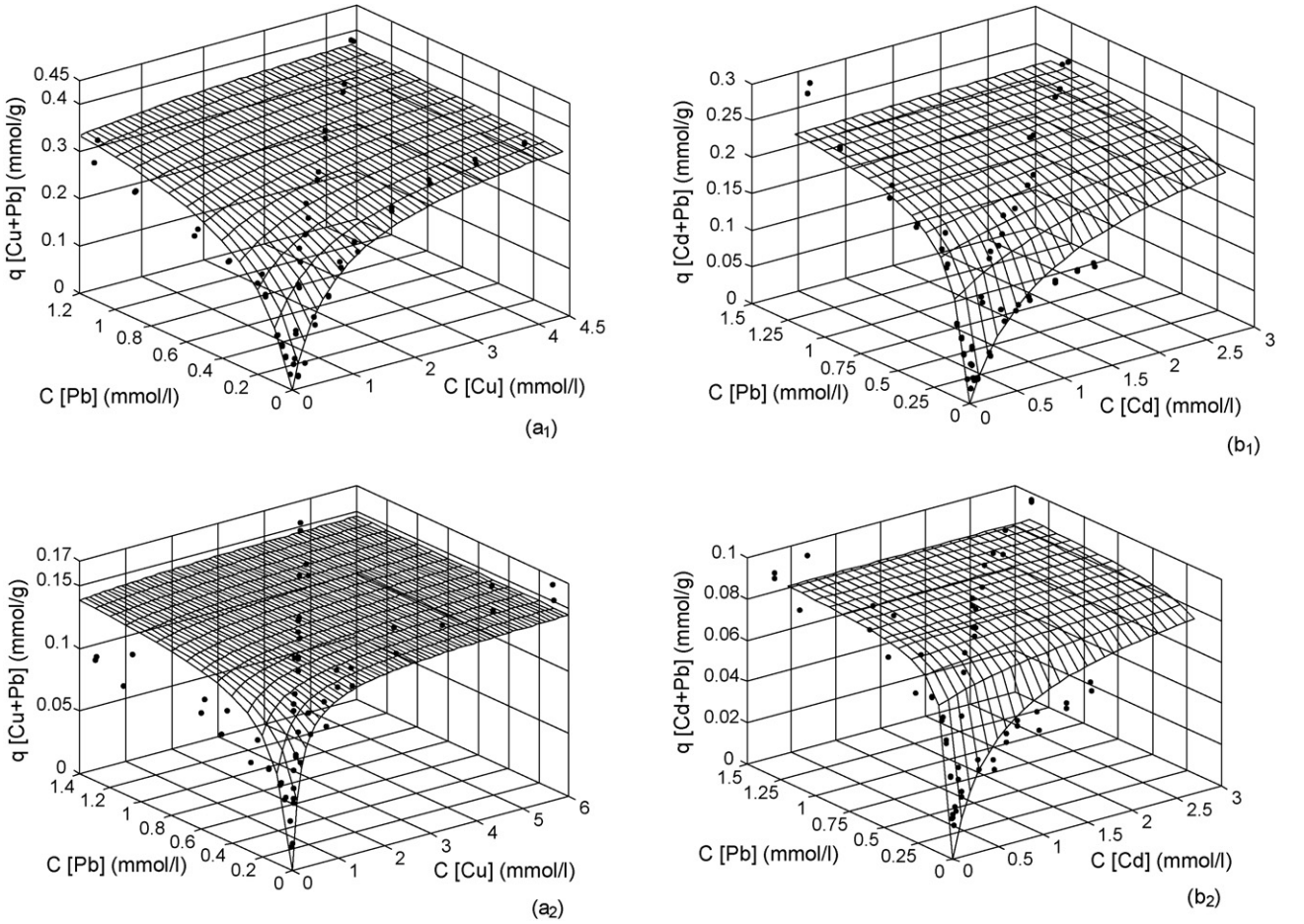

Fig. 1. Two-metal sorption isotherm surfaces for Pb/Cu (a_i) and Pb/Cd (b_i). The total metal uptake is plotted as a function of the equilibrium concentration in solution at pH 5.3 and 20 °C. (a_1) and (b_1)—Algae *Gelidium*, (a_2) and (b_2)—Composite material.

Table 1
Adjustable parameters for the multi-component discrete equilibrium model (value ± standard deviation)

Biosorbent	System	Metal	Discrete model			R^2	S_2^R (mmol/g)^2
			Q_{max} (mmol/g)	pK_M	pK_H		
Gelidium	Pb^{2+}/Cu^{2+}	Pb^{2+} Cu^{2+}	0.40 ± 0.01	3.63 ± 0.05 3.23 ± 0.05	4.21 ± 0.06	0.912	1.1×10^{-3}
	Pb^{2+}/Cd^{2+}	Pb^{2+} Cd^{2+}	0.28 ± 0.01	3.98 ± 0.05 3.16 ± 0.04	4.05 ± 0.05	0.926	4.3×10^{-4}
Composite material	Pb^{2+}/Cu^{2+}	Pb^{2+} Cu^{2+}	0.15 ± 0.01	4.2 ± 0.2 3.9 ± 0.2	4.9 ± 0.2	0.771	7.5×10^{-4}
	Pb^{2+}/Cd^{2+}	Pb^{2+} Cd^{2+}	0.098 ± 0.002	4.50 ± 0.05 3.42 ± 0.04	4.58 ± 0.05	0.924	6.0×10^{-5}

R^2, correlation coefficient; S_2^R, model residual variance.

concentration is 3.3 times higher than that of Pb(II), at the end of the experiments, were removed 0.483 and 1.81 mmol of Cu(II) (4.0 and 8.6 mg/g) and 0.18 and 0.64 mmol of Pb(II) (4.6 and 9.7 mg/g), respectively, for the composite material and algae *Gelidium* (Fig. 2(a and b)). Comparing the results with the obtained from single-metal solutions [24] in the same operating conditions, the copper uptake capacity in the presence of lead ions slightly decrease, but the presence of high initial copper concentration significantly reduce the lead ions uptake capacity (60–70%). Lower final pH values were obtained in biosorption from two-metal solutions, when compared with adsorption experiments from single-metal solutions [24]. As the pH decreases due to ion exchange between metal ions and protons from surface carboxylic groups [18,19,24], the higher initial metal concentration in the two-metal solution displaces more protons.

Fig. 2 compares the experimental data with the mass transfer model predicted curves. Simulation has been done using the model parameters from Table 3. The homogeneous diffusion coefficients were determined in a previous work [10]. Affinity constants, K_i, were calculated from Eq. (3), for the final pH value of the continuous experiment. Fig. 2 shows that the initial "knee" of the experimental curve is well predicted by the model curves. As shown in a previous work [24], the stirring velocity used in this system (270 rpm) is not enough to eliminate the external mass transfer resistance, which produces the "knee" in the breakthrough curves. The higher external mass transfer resistance was found for algae *Gelidium* particles. Simulation has been done assuming equilibrium parameters from batch experiments, inside the obtained confidence intervals.

$N_f < \xi N_d$ for algae *Gelidium*, suggesting that resistance in the film is more important than intraparticle diffusion resistance. The same behavior was found for Pb(II) adsorption in the composite material. For Cu(II) adsorption on the same adsorbent, $N_f > \xi N_d$, indicating that the intraparticle resistance is more important. Film coefficient values, k_f, are higher for the composite material, suggesting lower external resistance than in algae *Gelidium*. This resistance is related to the "knee" of the breakthrough curve.

After biosorbents saturation, biomass has been regenerated with 0.1 M HNO_3 solution. Comparing the area under the elution curves (Fig. 3) with the metal uptake until saturation, we conclude that desorption was very fast and 100% efficient. The same results have been obtained from one-metal desorption experiments [24].

The total desorption of Cu(II) from both biosorbents have not been achieved in the batch system, using the same concentration of eluent [18], because in column and CSTA experiments, the fresh eluent solution is continuously fed, resulting in a higher driving force for ion exchange between metal ions and protons [10,25].

Table 2
Operating parameters for the saturation and elution experiments (270 rpm and 20 °C)

Material	Experiment	Metal Type	Q (cm^3/min)	pH_{SE}	pH_{AI}	pH_{AE}	C_{E_i} / C_{AI} (mg/l)	$C_{final(i)}$ (mg/l)	W (g)	ε	τ (min)
Gelidium	1	S	35.5	5.4	5.7	4.4	Cu–25.1/0 Pb–24.4/0	Cu–23.0 Pb–21.0	13.7	0.978	14.9
	2	Pb/Cu E		1.2	4.5	1.2	Cu–0/23.0 Pb–0/21.0	Cu–0.7 Pb–0.6			
	3	Pb/CdS	35.5	5.3	5.4	4.6	Pb–26.1/0 Cd–28.1/0	Pb–20.7 Cd–26.5	14.4	0.980	14.9
Composite material	4	S	35.5	5.4	5.7	4.3	Cu–25.1/0 Pb–24.8/0	Cu–25.0 Pb–24.8	8.1	0.940	14.3
	5	Cu/Pb E		1.1	4.6	1.1	Cu–0/25.0 Pb–0/24.8	Cu–0.7 Pb–0.9			
	6	Pb/CdS	35.5	5.3	5.7	5.0	Pb–23.4/0 Cd–22.1/0	Pb–22.5 Cd–22.1	8.2	0.939	14.3

S, Saturation; E, Elution.

Table 3
Mass transfer parameters for Pb/Cu biosorption

Experiment	K_i (l/mmol)		Q_{max} (mmol/g)	ξ		ε	D_h (cm^2/s) × 10^8		K_f (cm/s) × 10^3		ξN_d		N_f	
	Cu	Pb		Cu	Pb		Cu	Pb	Cu	Pb	Cu	Pb	Cu	Pb
1	1.4	2.4	0.40	30.2	100.6	0.978	28	6	3	5	905.3	646.7	12.1	20.1
4	1.1	2.3	0.15	6.1	20.1	0.940	6.9	6.3	8	8	42.7	130.0	88.4	

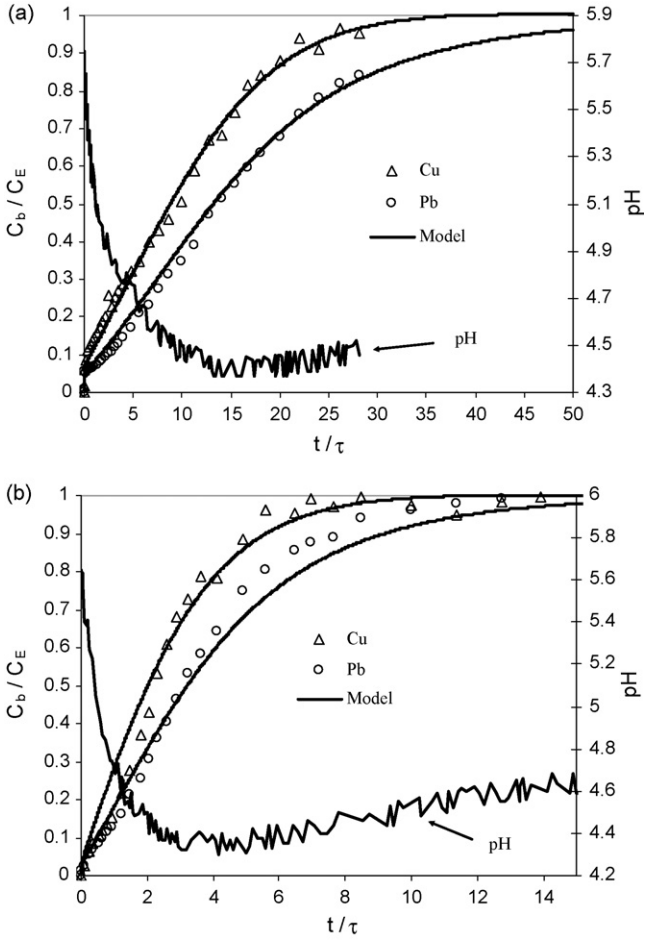

Fig. 2. Experimental data and simulated concentration profiles for continuous biosorption from a Pb/Cu solution: (a) algae *Gelidium* and (b) composite material.

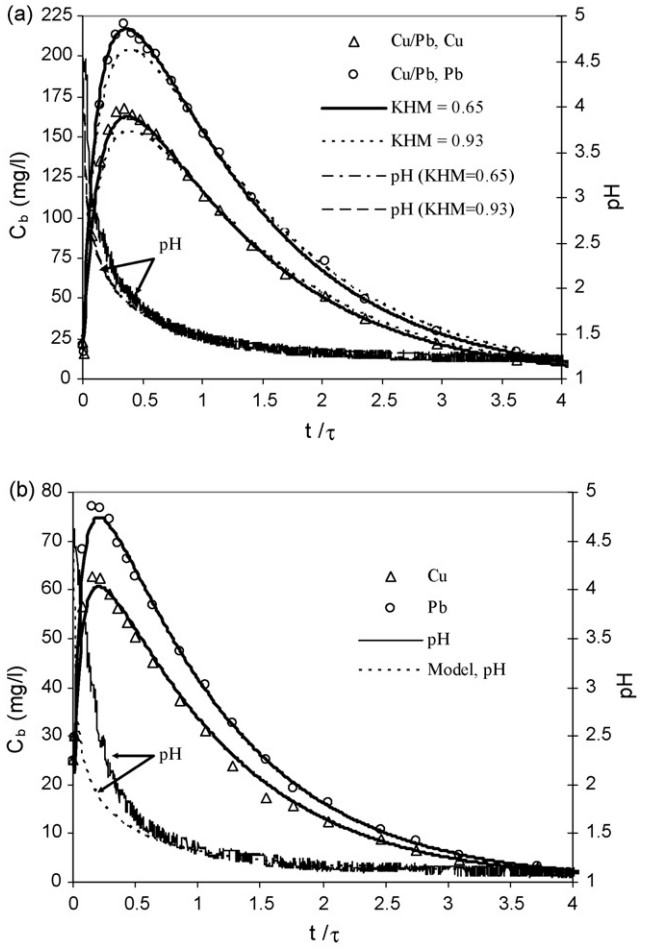

Fig. 3. Experimental data and simulated concentration profiles for continuous elution of adsorbed Pb/Cu: (a) algae *Gelidium* and (b) composite material.

The concentration ratio, CR (ratio between the higher metal concentration desorbed and the feed metal concentration in the saturation process) depends on the biomass adsorption properties. The Langmuir parameters (Q_{max} and K_i) are direct indicators of the CR potential. For a 100% efficient desorption process, CR values can be estimated for each metal ion by:

$$CR_i = \left(\frac{S}{L}\right) \frac{Q_{max} K_i}{1 + \sum_{i=1}^{2} K_i C_{final(i)}} \quad (24)$$

The equilibrium concentration in a batch system corresponds to the inlet concentration in the CSTA. The calculated CR, using

Table 4
Mass transfer parameters for elution of Pb/Cu

Experiment	$K_H^{Cu} = K_H^{Pb}$	Q_{max} (mmol/g)	ξ'		ε	D_h (cm^2/s) × 10^7		N_d		ξN_d	
			Cu	Pb		Cu	Pb	Cu	Pb	Cu	Pb
2	0.93, **0.65**	**0.36**	**19**		**0.978**	2.0, **5.0**		21.5, **53.7**		409, **1022**	
5	**1.1**	**0.16**	**4.8**		**0.939**	**4.0**		**41.2**		**196**	

Values used for the simulation in bold.

Table 5
Mass transfer parameters for Pb/Cd biosorption

Experiment	K_i (l/mmol)		Q_{max} (mmol/g)	ξ		ε	D_h (cm^2/s) $\times 10^8$		K_f (cm/s) $\times 10^3$		ξN_d		N_f	
	Cd	Pb		Cd	Pb		Cd	Pb	Cd	Pb	Cd	Pb	Cd	Pb
3	1.6	9.6	0.29	31.6	62.6	0.980	8.8	6.0	4	4	297	403.1	14.5	
6	2.0	17.0	0.098	8.1	14.0	0.939	5.0	6.3	4	3	41.8	95.7	44.7	33.6

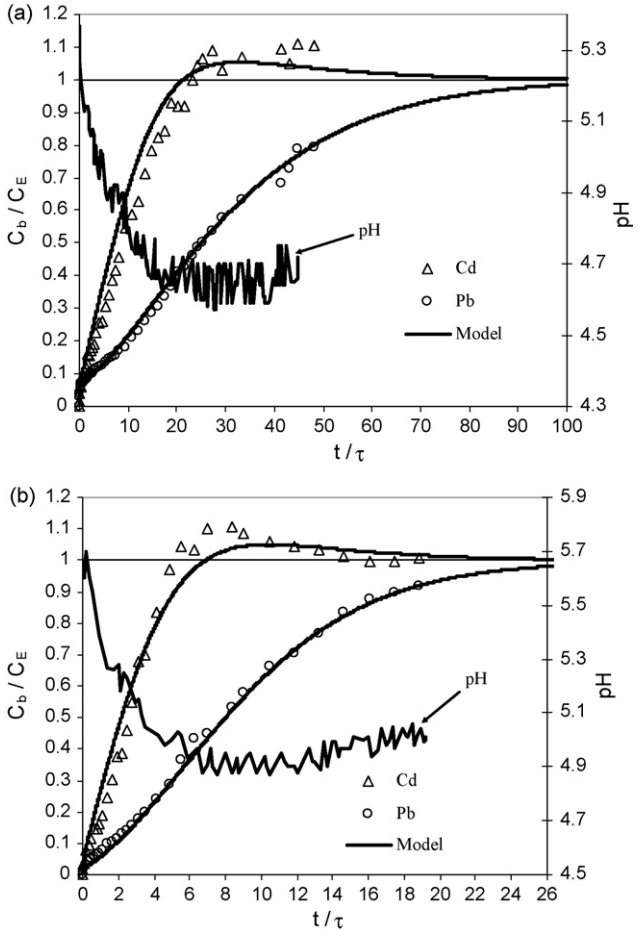

Fig. 4. Experimental data and simulated concentration profiles for continuous biosorption from a Pb/Cd solution: (a) algae *Gelidium* and (b) composite material.

equilibrium data and Eq. (24) are close to the experimental ones, suggesting that CR can be estimated from the equilibrium data, as it was concluded from single-metal adsorption experiments [24].

A mass transfer model, assuming intraparticle diffusion and the mass action law to describe the equilibrium, has been applied to the experimental desorption results.

Fig. 3 presents the experimental results and simulated curves. The model fits the experimental data, with the same homogeneous diffusion coefficient for both metal ions (Table 4) and close to those obtained from single-metal adsorption experiments [24]. For algae *Gelidium*, the best fitting was obtained for lower K_H^M values ($K_H^{Cu} = K_H^{Pb} = 0.65$), than the obtained from batch experiments [18]. The high $\xi' N_d$ values suggest that metal ions diffusion from the solid phase to the bulk solution is very fast, due to the high proton diffusivities. Fig. 3 also presents the pH profiles inside the adsorber and the simulated curves. The good agreement obtained between simulated and experimental results suggests that the elution mechanism is essentially ion exchange between protons and metal ions.

4.2.2. Biosorption from Pb/Cd solution

Fig. 4 represents the biosorption results from a Pb/Cd solution. After being initially adsorbed, the Cd(II) is progressively substituted by Pb(II), producing an "overshoot" region in the breakthrough curves. This is the result of the higher Pb(II) affinity for the binding sites and competition with previously bounded Cd(II). So, the total cadmium uptake has been computed discounting cadmium ions released to the solution. For the composite material, were initially adsorbed 26.3 mg of Cd and were released 12.2 mg Cd to the solution, which were substituted by Pb(II). Although the inlet cadmium concentration is around 2 times higher than lead concentration, more Pb(II) have been removed, given its higher affinity for the binding sites ($K_{Pb}/K_{Cd} = 6.5$ and 11.3, respectively, for algae *Gelidium* and composite material).

Fig. 4 also presents simulated curves by the mass transfer model and the respective parameters are listed in Table 5. The simulated curves fit well the experimental breakthrough, showing that film diffusion is an important step in the biosorption process, in agreement with $\xi N_d > N_f$ (Table 5). The exception is the biosorption of Cd(II) onto the composite material, when $\xi N_d \approx N_f$. Simulation has been done using equilibrium parameters from batch experiments, inside the obtained confidence intervals.

The parameter $X_m^2(r_{cryst} + 0.85)$ has been introduced by Nieboer and McBryde [26] as a measure of the covalent binding strength, where 0.85 stands for the contribution of N or O donors to the bind distance and r_{cryst} is the Shannon crystal radii. "Hard" ions are characterized by $X_m^2(r_{cryst} + 0.85) <\approx 4.2$, and "soft" ions by $X_m^2(r_{cryst} + 0.85) > 7$. The $X_m^2(r_{cryst} + 0.85)$ criterion confirms that the relative contribution of covalent binding follows the order Pb (6.61) > Cu (6.32) > Cd (5.20) and that cadmium has a lower affinity to the binding sites than Pb and Cu. The criterion also suggests higher competition of Pb(II) with Cu(II) than with Cd(II), in accordance with he experimental results.

5. Conclusions

Experimental data for binary metal biosorption (Pb/Cd and Pb/Cu) in a CSTA, showed a higher affinity of the binding sites present in the surface of the biosorbents for Pb(II) than for Cu(II) and Cd(II). Mass transfer models for the biosorption and

desorption were developed for the design of continuous biosorption processes in CSTA. These models were able to predict the experimental data for biosorption and desorption steps of binary systems. It was concluded that the initial "knee" in the biosorption breakthrough curve was due the mass film resistance. The desorption step was 100% efficient and fast, using a 0.1 M HNO_3 solution as eluent.

Acknowledgements

Financial support for this work was in part provided by national research grant FCT/POCTI/AMB/57616/2004 and by LSRE financing by FEDER/POCI/2010, for which the authors are thankful. V. Vilar's acknowledges his Ph.D. scholarship by FCT (SFRH/BD/7054/2001).

References

[1] B. Volesky, Sorption and Biosorption, first ed., BV Sorbex, Inc., Quebec, 2003.
[2] J. Wase, C. Forster, Biosorbents for Metal Ions, Taylor & Francis, London, 1997.
[3] T.A. Davis, B. Volesky, A. Mucci, A review of the biochemistry of heavy metal biosorption by brown algae, Water Res. 37 (2003) 4311–4330.
[4] M. Ajmal, A.H. Khan, S. Ahmad, A. Ahmad, Role of sawdust in the removal of copper(II) from industrial wastes, Water Res. 32 (10) (1998) 3085–3091.
[5] N. Mameri, N. Boudries, L. Addour, D. Belhocine, H. Lounici, H. Grib, A. Pauss, Batch zinc biosorption by a bacterial nonliving *Streptomyces rimosus* biomass, Water Res. 33 (6) (1999) 1347–1354.
[6] M.Y. Arica, Y. Kaçar, Ö. Genç, Entrapment of white-rot fungus *Trametes versicolor* in ca-alginate beads: preparation and biosorption kinetic analysis for cadmium removal from an aqueous solution, Biores. Technol. 80 (2001) 121–129.
[7] S.E. Bailey, T.J. Olin, R.M. Bricka, D.D. Adrian, A review of potentially low-cost sorbents for heavy metals, Water Res. 33 (11) (1999) 2469–2479.
[8] S. Babel, T.A. Kurniawan, Low-cost adsorbents for heavy metals uptake from contamined water: a review, J. Hazard. Mater. B97 (2003) 219–243.
[9] A.K. Bhattacharya, C. Venkobachar, Removal of cadmium(II) by low cost adsorbents, J. Environ. Eng. 110 (1) (1984) 110–122.
[10] V.J.P. Vilar, Uptake of metal ions in aqueous solution by algal waste from agar extraction industry, Ph.D. Thesis, Faculty of Engineering University of Porto, Porto, 2006.
[11] V.J.P. Vilar, C.M.S. Botelho, R.A.R. Boaventura, Influence of pH, ionic strength and temperature on lead biosorption by *Gelidium* and agar extraction algal waste, Proc. Biochem. 40 (10) (2005) 3267–3275.
[12] V.J.P. Vilar, C.M.S. Botelho, R.A.R. Boaventura, Equilibrium and kinetic modelling of Cd(II) biosorption by algae *Gelidium* and agar extraction algal waste, Water Res. 40 (2) (2006) 291–302.
[13] V.J.P. Vilar, C.M.S. Botelho, R.A.R. Boaventura, Copper removal by algae *Gelidium*, agar extraction algal waste and granulated algal waste: Kinetics and equilibrium, Biores. Technol. 99 (2008) 750–762.
[14] V.J.P. Vilar, F. Sebesta, C.M.S. Botelho, R.A.R. Boaventura, Equilibrium and kinetic modelling of Pb^{2+} biosorption by granulated agar extraction algal waste, Proc. Biochem. 40 (10) (2005) 3276–3284.
[15] Y. Sag, A. Yalcuk, T. Kutsal, Mono and multi-component biosorption of heavy metal ions on *Rhizopus arrhizus* in a CSFT, Proc. Biochem. 35 (8) (2000) 787–799.
[16] F. Beolchini, F. Pagnanelli, L. Toro, F. Vegliò, Continuous biosorption of copper and lead in single and binary systems using *Sphaerotilus natans* cells confined by a membrane: experimental validation of dynamic models, Hydrometallurgy 76 (2005) 73–85.
[17] F. Pagnanelli, F. Beolchini, A.D. Biase, F. Vegliò, Biosorption of binary heavy metal systems onto *Sphaerotilus natans* cells confined in an UF/MF membrane reactor: dynamic simulations by different Langmuir-type competitive models, Water Res. 38 (2004) 1055–1061.
[18] V.J.P. Vilar, C.M.S. Botelho, R.A.R. Boaventura, Copper desorption from *Gelidium* algal biomass, Water Res. 41 (7) (2007) 1569–1579.
[19] V.J.P. Vilar, C.M.S. Botelho, R.A.R. Boaventura, Kinetics and equilibrium modelling of lead uptake by algae *Gelidium* and algal waste from agar extraction industry, J. Hazard. Mater. 143 (1–2) (2007) 396–408.
[20] V.J.P. Vilar, C.M.S. Botelho, R.A.R. Boaventura, Methylene blue adsorption by algal biomass based materials: biosorbents characterization and process behaviour, J. Hazard. Mater. 127 (1–2) (2007) 120–132.
[21] A.C. Hindmarsh, Odepack, A Systematized Collection of ODE Solvers, in Scientific Computing, Scientific Computing, Amsterdam, 1983.
[22] D.G. Kinniburgh, W.H.V. Riemsdijk, L.K. Koopal, M. Borkovec, M.F. Benedetti, M.J. Avena, Ion binding to natural organic matter: Competition, heterogeneity, stoichiometry and thermodynamic consistency, Colloids Surf. A 151 (1999) 147–166.
[23] R. Sips, On the structure of a catalyst surface, J. Chem. Phys. 16 (1948) 490–495.
[24] V.J.P. Vilar, C.M.S. Botelho, R.A.R. Boaventura, Lead and copper biosorption by marine red algae *Gelidium* and composite material in a CSTR ("Carberry" Type), Chem. Eng. J. 138 (2008) 249–257.
[25] R.H. Crist, J.R. Martin, D.R. Crist, Interaction of metals and protons with algae Equilibrium constants and ionic mechanisms for heavy metal removal as sulfides and hydroxides, in: R.W. Smith, M. Misra (Eds.), Mineral bioprocessing, The Minerals, Metals and Materials Society, Washington, DC, 1991, pp. 275–287.
[26] E. Nieboer, W.A.E. McBryde, Free-energy relationship in coordination chemistry. III. A comprehensive index to complex stability, Can. J. Chem. 51 (1973) 2512–2524.